Critical Properties of Four HFE + HFC Binary Systems: Trifluoromethoxymethane (HFE-143m) + Pentafluoroethane (HFC-125), + 1,1,1,2-Tetrafluoroethane (HFC-134a), + 1,1,1,2,3,3,3-Heptafluoropropane (HFC-227ea), and + 1,1,1,2,3,3-Hexafluoropropane (HFC-236ea)

Yuko Uchida,[†] Masahiko Yasumoto,[‡] Yasufu Yamada,[§] Kenji Ochi,[†] Takeshi Furuya,[‡] and Katsuto Otake*,[‡,||]

College of Science & Technology, Nihon University, Kanda-Surugadai 1-8-14, Chiyoda-ku, Tokyo 101-8308, Japan, National Institute of Advanced Industrial Science and Technology, Nanotechnology Research Institute, Higashi 1-1-1, Tsukuba Central 5, Tsukuba, Ibaraki 305-8565, Japan, Daikin Industries, Ltd., Umeda-Center Building, 2-4-12, Nakazaki-Nishi, Kita-Ku, Osaka 530-8323, Japan and National Institute of Advanced Industrial Science and Technology, Research Center for Developing Fluorinated Greenhouse Gas Alternatives, Higashi 1-1-1, Tsukuba Central 5, Tsukuba, Ibaraki 305-8565, Japan

Trifluoromethoxymethane (CF_3OCH_3, HFE-143m) is a promising alternative for dichlorodifluoromethane (CCl_2F_2, CFC-12) as a refrigerant. Because of its low flammability, it is expected to be used in binary mixtures with inflammable hydrofluorocarbons (HFCs). In this study, we measured the critical parameters of binary mixtures of HFE-143m with four HFCs—pentafluoroethane (CHF_2CF_3, HFC-125), 1,1,1,2-tetrafluoroethane (CH_2FCF_3, HFC-134a), 1,1,1,2,3,3,3-heptafluoropropane (CF_3CHFCF_3, HFC-227ea), and 1,1,1,2,3,3-hexafluoropropane (CHF_2CHFCF_3, HFC-236ea). The uncertainties were ±10 mK in temperature, ±0.5 kPa in pressure, ±1 kg m^{-3} in density, and ±0.5% in composition (molar base). The HFCs were selected for the similarities of their normal boiling points. The experimental data were correlated with equations proposed by Higashi.

1. Introduction

Chlorofluorocarbons (CFCs) have been utilized extensively as refrigerants, blowing agents, and cleaning solvents because of their chemical stability and physical properties. However, they have been identified as contributing to ozone layer depletion and global warming, and their use has been restricted. They were replaced by alternative CFCs (HCFCs and HFCs). Unfortunately, they too are required to be restricted by 2020. Furthermore, the HFCs have also been identified as greenhouse gases in the Kyoto Protocol and will be banned soon. The development of new alternatives has thus become a matter of urgency.

Hydrofluoroethers (HFEs) are environmentally benign compounds having zero ODP and low GWP and are expected to be the new alternatives.[1,2] The Research Institute of Innovative Technology for the Earth (RITE) synthesized and evaluated about 150 HFEs.[3,4] Of these, trifluoromethoxymethane (CF_3OCH_3, HFE-143m) and pentafluoromethoxyethane ($CF_3CF_2OCH_3$, HFE-245mc) were found to be possible alternatives for dichlorodifluoromethane (CCl_2F_2, CFC-12) and 1,2-dichloro-1,1,2,2-tetrafluoroethane ($CClF_2CClF_2$, CFC-114), respectively. The physical properties of HFE-143m and HFE-245mc are summarized in Table 1.[3–5] As shown in the Table, they are slightly combustible (ASHRAE class 2). Thus, for safety reasons,

the HFEs are expected to be used in binary mixtures with inflammable HFCs.

The critical properties (critical temperature, pressure, and density) are the most important physical properties for the development of an equation of state to calculate and estimate the thermodynamic properties of fluids in industry. However, reliable information on the thermophysical properties of these mixtures has not yet been reported. In previous papers, we described an apparatus for the precise measurement of critical properties and its application to the newly synthesized HFEs, hydrofluoroketones, and a hydrofluoroamine.[6,7] In the present article, using this apparatus, we measured the critical parameters of binary mixtures of HFE-143m and pentafluoroethane (CHF_2CF_3, HFC-125), 1,1,1,2-tetrafluoroethane (CH_2FCF_3, HFC-134a), 1,1,1,2,3,3,3-heptafluoropropane (CF_3CHFCF_3, HFC-227ea), and 1,1,1,2,3,3-hexafluoropropane (CHF_2CHFCF_3, HFC-236ea).

2. Experimental Section

Materials. Table 2 summarizes the sample codes, molecular formulas, molar based purities, and normal boiling points for all of the compounds used in this study. They were all supplied by RITE. Their molar-based purities were analyzed by gas chromatography (Hewlett-Packard, model HP-6890; thermal conductivity detector). The critical parameters of these compounds are given in Table 3. In previous work, extreme care was taken to remove all traces of water from the samples because it is known to initiate the decomposition of samples.[31] In this study, all compounds are thermally stable, and dehydration procedures were not employed.

* Corresponding author. E-mail: katsuto-otake@aist.go.jp. Phone: +81-298-61-4567 or +81-298-61-4819. Fax: +81-298-61-4567.
[†] Nihon University.
[‡] National Institute of Advanced Industrial Science and Technology.
[§] Daikin Industries, Ltd.
[||] National Institute of Advanced Industrial Science and Technology.

Table 1. Properties of HFE-143m and HFE-245mc

	HFE-143m (CF_3OCH_3)	HFE-245mc ($CF_3CF_2OCH_3$)
life time /year	4.9	4.5
global warming potential ITH = 20	2200	1800
= 100	680	530
= 500	210	170
normal boiling point/K	249.15	279.05
acentric factor/−	0.282	0.353
vapor pressure (at 298.15 K)/MPa	0.576	0.206
density (saturated liquid at 298.15 K)/kg m^{-3}	109.4	126.6
heat of vaporization (at 298.15 K)/kJ kg^{-1}	173.3	166.0
C_p (saturated liquid, 296.15 K)/kJ K kg^{-1}	1.416	1.296
viscosity (saturated liquid, 298.15K)/mPa s	0.196	0.277
heat conductivity (saturated liquid, 296.15 K)/W K m^{-1}	0.0762	0.0696
surface tension (saturated liquid, 296.15 K)/dyn cm^{-1}	8.21	10.01
solubility to water (saturated liquid, 296.15 K)/g (100 g)$^{-1}$	0.057	0.020
dielectric constant (saturated liquid, 296.15 K)/−	9.5	7.3
heat of combustion/kJ mol^{-1}	757	950
combustion range/vol %	10.5−21.5	10.5−13.5
ASHRAE class	2	2

Table 2. Compounds Used in This Study

sample code	molecular formula	name	CAS RN	purity[a]	boiling point/K[3,4]
HFE-143m	CF_3OCH_3	trifluoromethoxymethane	421-14-7	99.9	249.15
HFC-125	CHF_2CF_3	pentafluoroethane	354-33-6	99.8	224.65
HFC-134a	CH_2FCF_3	1,1,1,2-tetrafluoroethane	811-97-2	99.99	246.6
HFC-227ea	CF_3CHFCF_3	1,1,1,2,3,3,3-heptafluoropropane	431-89-0	99.8	257.65
HFC-236ea	CHF_2CHFCF_3	1,1,1,2,3,3-hexafluoropropane	431-63-0	99.4	277.65

[a] Measured in this study.

Table 3. Critical Parameters of the Compounds Used in This Study

	author	T_C/K	P_C/MPa	ρ_C/kg·m^{-3}	reference
HFE-143m (CF_3OCH_3)	Wang et al.	378.0	3.680	439	8[a]
	Salivi-Narkhede	378.02	3.588	439	9[a]
	Yoshii et al.	377.901		464	10[a]
	Widiatmo et al.		3.649		11[a]
	Widiatmo et al.		3.640		12[a]
	this work	377.92	3.640	459	
HFC-125 (CHF_2CF_3)	Wilson et al.	339.19	3.595	571.3	13[a]
	Schmidt et al.	339.33		565	14[a]
	Kuwabara et al.	339.165		568	15[a]
	Nagel et al.	339.43	3.635	567.7	16[a]
	Higashi	339.17	3.620	577	17[a], 26[a]
	REFPLOP	339.33	3.629	571.3	18[b]
	Span et al.	339.33	3.629	571.3	19[b]
	this work	339.20	3.617	560	
HFC-134a (CH_2FCF_3)	Maezawa et al.	374.30		508	20[a]
	Baehr et al.	374.18	4.058		21[a]
	JAR & JFGA	374.30	4.065	511	22[b]
	Stroem et al.	374.25	4.070		23[a]
	Aoyama et al.	374.08		509	24[a]
	Fujiwara et al.	374.07	4.050	509	25[a]
	Higashi	374.11		508	26[a]
	Span et al.	374.18	4.056	508.0	19[b]
	this work	374.13	4.053	508	
HFC-227ea (CF_3CHFCF_3)	Salvi-Narkhede et al.	374.83	2.9116	626	9[a]
	McLinden et al.	374.89	2.9290		18[b]
	Shi et al.	375.95	2.9877		27[a]
	Defibaugh et al.	375.95	2.9346	580	28[a]
	this work.	375.00	2.930	598	
HFC-236ea (CHF_2CHFCF_3)	Zhang et al.		3.412		30[a]
	Aoyama et al.	412.375		568	24[a]
	Defibaugh et al.	412.44	3.501	563	29[a]
	Huber et al.	412.44	3.502	563	18[b]
	this work	412.41	3.416	562	

[a] Experimental data. [b] Recommended or estimated data.

Apparatus. The critical points of the mixtures were measured by observing the behavior of the meniscus at the vapor−liquid interface in an optical cell. Figure 1 is a schematic representation of the experimental apparatus. The apparatus is composed of four main parts: a rectangularly shaped optical cell (A, ca. 5 cm^3 in volume), two variable-volume vessels to control the inner volume of the apparatus (B), a differential null-pressure detector (C), and
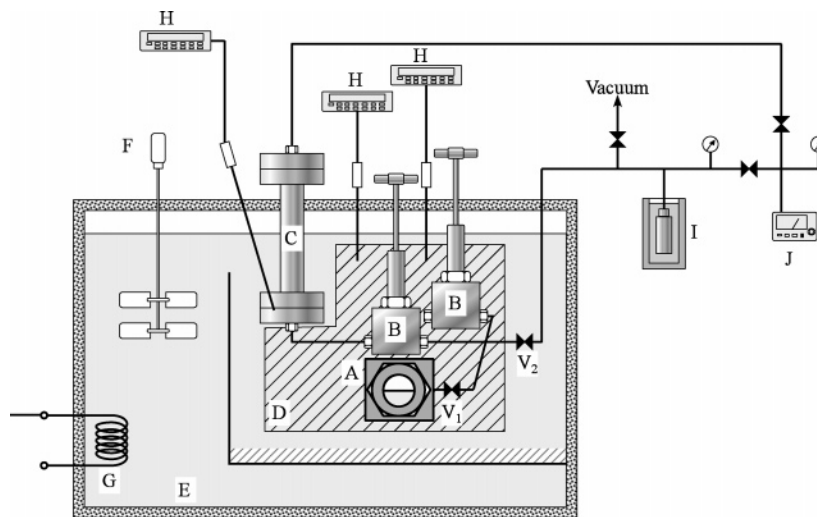
Figure 1. Experimental apparatus. A, Optical cell; B, variable-volume vessel; C, differential null-pressure detector; D, aluminum blocks; E, constant-temperature oil bath; F, impeller; G, temperature controller; H, platinum resistance thermometer; I, cold trap; J, quartz crystal pressure gauge; V_1, cutoff valve; and V_2, separation valve.
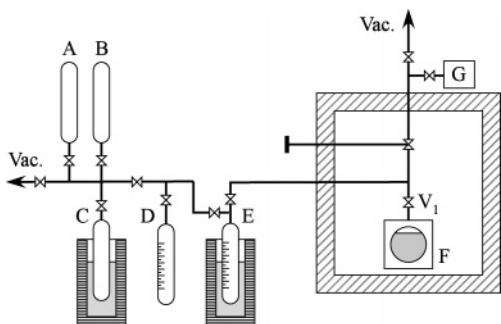
Figure 2. Apparatus for sample loading. A, Stainless steel sample cylinder for component 1; B, stainless steel sample cylinder for component 2; C, stainless steel cylinder for purification; D and E, glass cylinders for purification and volume measurement; F, optical cell; and G, pressure gauge.

aluminum blocks (D) that acted as thermal masses to minimize temperature fluctuations. The optical cell was connected to the two variable-volume vessels and the differential null-pressure detector by a valve (V_1). The central axis of these vessels and the detector were adjusted to be at the same level. The temperature of the oil bath was controlled to within ±3 mK in the range of (300 to 450) K. Under these conditions, the uncertainty in the critical temperature is estimated to be ±10 mK. The uncertainties in pressure and density were estimated to be less than ±0.5 kPa and ±1 kg m^{-3}, respectively. The apparatus was specially designed for the critical parameter measurements with small sample sizes and needs only (5 to 6) mL for a single experiment. A detailed description of the experimental apparatus was given in the previous papers.[6,7]

Procedure. (a) Sample Loading. To prepare the desired composition of mixtures for investigation, the apparatus shown in Figure 2 was used. Stainless steel sample cylinders A (containing sample 1) and B (containing sample 2) were connected to the apparatus, and the apparatus was evacuated. Sample A was transferred to stainless steel cylinder C and to glass cylinder D under vacuum by using hot water and liquid nitrogen to remove dissolved gas. Cylinder D was disconnected, weighed, and connected again, and the apparatus was re-evacuated. Sample B was then transferred to cylinder C and to cylinder D similarly to make the final mixture in cylinder D. Cylinder D was disconnected, weighed, and connected

again, and the sample mixture in cylinder D was transferred to cylinder E and loaded into the optical cell situated in a constant-temperature air bath at 233 K under vacuum. After (80 to 90)% of the optical cell was filled with the liquid mixture, the cell was disconnected from the apparatus at valve V_1 and connected to the critical parameters measurement apparatus shown in Figure 1. The initial composition of the sample mixture was calculated from the weight ratio of pure samples in cylinder D.

(b) Critical Parameters Measurement. After the optical cell was connected to the main apparatus (Figure 1, at V_1), the remaining part of the apparatus was evacuated. Valve V_2 was closed, and the temperature was raised to the desired value. After the temperature fluctuations became less than ±5 mK, V_1 was opened to fill the apparatus. The position of the meniscus was controlled by the variable-volume vessels to be (1 to 2) mm above the center of the optical windows. At this stage, time was allowed for the pressure fluctuations to become less than ±0.1 kPa. After the temperature and the pressure became stable, they were recorded, and V_1 was closed.

After completing this sequence, the temperature was raised in 10 K increments. After the temperature fluctuations became less than ±5 mK, which sometimes required several hours, V_1 was opened, the position of the meniscus being maintained by the variable-volume vessel, and time was allowed for the pressure fluctuation to become less than ±0.1 kPa. After the temperature and the pressure became stable, they were recorded, and V_1 was closed. These procedures—increase in temperature, temperature stabilization period, opening V_1, control of the position of the meniscus, pause for pressure stabilization, recording of the temperature and pressure, and closing V_1—were repeated until near the critical condition. In this study, because it deals with binary systems, a minute temperature difference between the null pressure detector and the optical cell may cause a difference in composition. The procedures described above were especially developed to minimize the inevitable composition differences between the optical cell and null pressure detector.

Near the critical temperature, when critical opalescence began to appear, the temperature increment was decreased to (10 to 5) mK. For each change in the temperature, more than 1 h of equilibration time was allowed, the density inside the optical cell was adjusted by the variable-volume
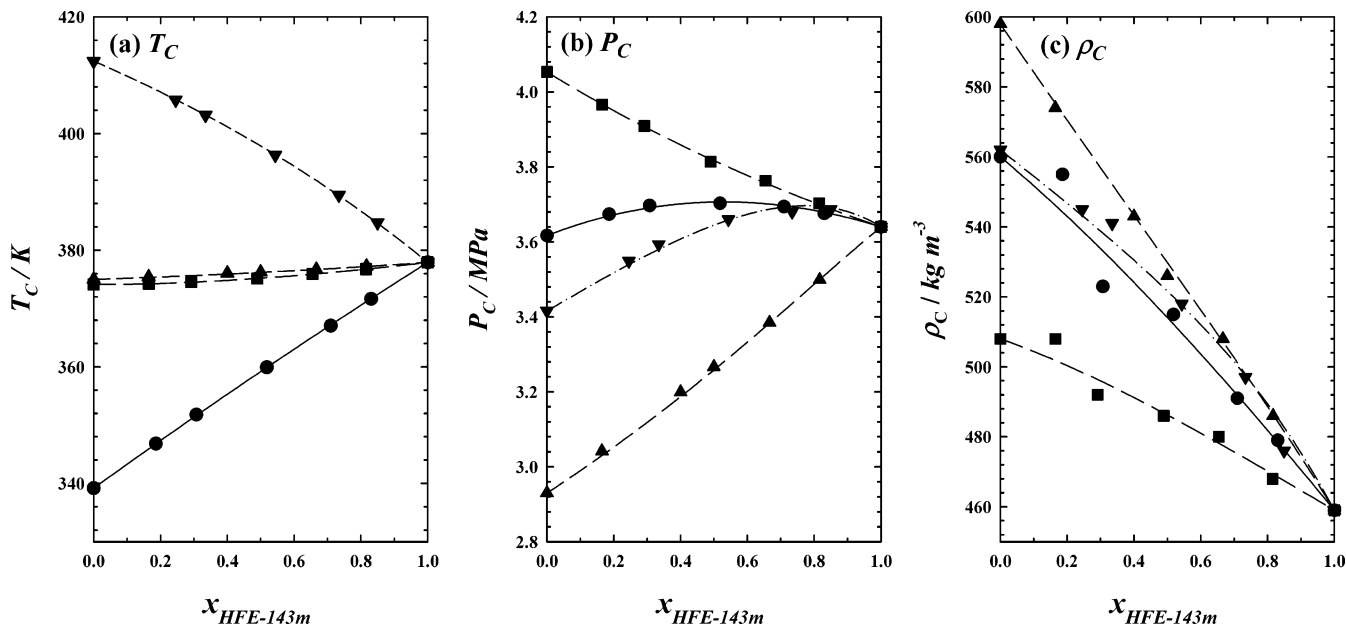
Figure 3. Critical parameters of the binary mixtures of HFE-143m and HFCs. (a) Critical temperature, (b) critical pressure, and (c) critical density: ●, HFC-125; ■, HFC-134a; ▲, HFC-227ea; and ▼, HFC-236ea. Lines are the correlated results of eqs 1 to 6: —, HFC-125; – – –, HFC-134a; - - -, HFC-227ea; and − · − · −, HFC-236ea.

vessels to give an equally strong critical opalescence in both the gas and the liquid phases, and the temperature and pressure were recorded. These procedures were repeated with a fine adjustment of the position of the meniscus until the temperature exceeded the critical temperature T_{CH} at which the meniscus disappears, while keeping equally strong critical opalescence to appear in both the gas and the liquid phases. In all of the procedures described above, V_1 is always closed except for the time when the temperature fluctuation is smaller than 5 mK.

Once the temperature exceeds T_{CH}, the temperature is set to 5 K higher than T_{CH} and kept constant for (4 to 20) h with V_1 open to achieve identical compositions in the optical cell and the null pressure detector. After the equilibration of the composition, temperature was decreased slowly to observe the reappearance of the meniscus at temperature T_{CL}. Then at a temperature between T_{CH} and T_{CL}, V_1 is closed, and another determination of the critical temperature is conducted. The critical pressure was calculated from a linear interpolation of the $p-T$ curve near the critical point. These procedures were repeated twice.

After the critical parameters measurements, the samples inside the optical cell and the null pressure detector were trapped in the cold trap (Figure 1, I) separately and weighed. The critical density was then determined from the mass of the sample and the known internal volume of the optical cell.

Procedures for the critical parameters measurements of pure substances were described in the previous papers.[6,7]

(c) Composition Analysis. As described above, minute temperature differences between the null pressure detector and the optical cell may cause a difference in composition. Because the critical temperature is measured by the behavior of the meniscus in the optical cell and the critical pressure is determined by the null pressure detector separated from the optical cell by valve V_1, if the composition between the optical cell and null pressure detector is different, then the measured critical parameters will include some errors. Thus, after the experiment, the composition of the samples in the null pressure detector and the optical cell were analyzed by gas chromatography

(Hewlett-Packard, model HP-6890; thermal conductivity detector) The uncertainty in the composition analysis was less than 0.2%. As will be described in the Results and Discussion section below, the composition difference is within 2.6% at the maximum.

(d) Correlation. Higashi proposed the following equations to correlate the critical parameters of binary HFC mixtures:[17,31]

$$T_{Cm} = \theta_1 T_{C1} + \theta_2 T_{C2} + 2\theta_1\theta_2\Delta_T \tag{1}$$

$$V_{Cm} = \theta_1 V_{C1} + \theta_2 V_{C2} + 2\theta_1\theta_2\Delta_V \tag{2}$$

$$P_{Cm} = \theta_1 P_{C1} + \theta_2 P_{C2} + 2\theta_1\theta_2\Delta_P \tag{3}$$

$$\rho_{Cm} = \frac{M_m}{V_{Cm}} \tag{4}$$

$$M_m = x_1 M_1 + (1 - x_1)M_2 \tag{5}$$

$$\theta_i = \frac{x_i V_{Ci}^{2/3}}{\displaystyle\sum_{j=1}^{2} x_j V_{Cj}^{2/3}} \qquad i = 1, 2 \tag{6}$$

where T_{Ci}, V_{Ci}, and P_{Ci} are the critical temperature, critical molar volume, and critical pressure of component i, respectively, x is the mole fraction, M_i is the molecular weight of component i, ϑ_i is the surface ratio of component i given by eq 6, and Δ_T, Δ_V, and Δ_P are the fitting parameters for critical temperature, volume, and pressure, respectively. Subscript m means mixture. Experimental data obtained in this study are correlated with the equations.

3. Results and Discussion

Critical Parameters of Mixtures. The critical parameters of pure substances used in this study are summarized in Table 3 together with literature data. All measured values fell within the range of other reports, thus confirming the reliability of the apparatus. Procedures for the measurements of pure components can be found elsewhere.[6,7]

Table 4. Critical Parameters of HFE-143m (1) + HFC-125 (2) Systems

$x_1{}^a$	T_C/K	P_C/MPa	ρ_C/kg m^{-3}	$x_1{}^b$ (optical cell base deviation/%)^d	$x_1{}^c$ (optical cell base deviation/%)^e
0.0000	339.20	3.617	560	0.0000 (0.00)	0.0000 (0.00)
0.1859	346.83	3.674	555	0.1753 (5.70)	0.1810 (2.64)
0.3073	351.78	3.697	523	0.2945 (4.17)	0.3028 (1.48)
0.5185	359.94	3.703	515	0.5066 (2.30)	0.5188 (−0.06)
0.7094	367.06	3.694	491	0.6962 (1.86)	0.7061 (0.47)
0.8305	371.66	3.676	479	0.8218 (1.05)	0.8275 (0.36)
1.0000	377.92	3.640	459	1.0000 (0.00)	1.0000 (0.00)
			AAD/%	(2.15)	(0.71)

^{a} Molar-based composition in the optical cell. ^{b} Molar-based composition calculated from the mass ratio. ^{c} Molar-based composition in the null pressure detector. ^{d} $100(x_{\text{optical cell}} - x_{\text{feed}})/x_{\text{optical cell}}$. ^{e} $100(x_{\text{optical cell}} - x_{\text{null pressure detector}})/x_{\text{optical cell}}$.

Table 5. Critical Parameters of HFE-143m (1) + HFC-134A (2) Systems

$x_1{}^a$	T_C/K	P_C/MPa	ρ_C/kg m^{-3}	$x_1{}^b$ (optical cell base deviation/%)^d	$x_1{}^c$ (optical cell base deviation/%)^e
0.0000	374.13	4.053	508	0.0000 (0.00)	0.0000 (0.00)
0.1649	374.25	3.966	508	0.1646 (0.18)	0.1654 (−0.30)
0.2914	374.56	3.909	492	0.2895 (0.65)	0.2892 (0.76)
0.4897	375.15	3.814	486	0.4889 (0.16)	0.4894 (0.06)
0.6543	375.94	3.763	480	0.6541 (0.03)	0.6540 (0.05)
0.8151	376.76	3.703	468	0.8154 (−0.04)	0.8167 (−0.20)
1.0000	377.92	3.640	459	1.0000 (0.00)	1.0000 (0.00)
			AAD/%	0.15	0.20

^{a} Molar-based composition in the optical cell. ^{b} Molar-based composition calculated from the mass ratio. ^{c} Molar-based composition in the null pressure detector. ^{d} $100(x_{\text{optical cell}} - x_{\text{feed}})/x_{\text{optical cell}}$. ^{e} $100(x_{\text{optical cell}} - x_{\text{null pressure detector}})/x_{\text{optical cell}}$.

Table 6. Critical Parameters of HFE-143m (1) + HFC-227ea (2) Systems

$x_1{}^a$	T_C/K	P_C/MPa	ρ_C/kg m^{-3}	$x_1{}^b$ (optical cell base deviation/%)^d	$x_1{}^c$ (optical cell base deviation/%)^e
0.0000	375.00	2.930	598	0.0000 (0.00)	0.0000 (0.00)
0.1647	375.41	3.042	574	0.1661 (−0.85)	0.1655 (−0.49)
0.3999	376.05	3.199	543	0.4075 (−1.90)	0.3985 (0.35)
0.4999	376.24	3.267	526	0.5002 (−0.06)	0.4985 (0.28)
0.6664	376.70	3.385	508	0.6684 (−0.30)	0.6661 (0.05)
0.8165	377.25	3.499	486	0.8157 (−0.10)	0.8153 (−0.15)
1.0000	377.92	3.640	459	1.0000 (0.00)	1.0000 (0.00)
			AAD/%	0.46	0.19

^{a} Molar-based composition in the optical cell. ^{b} Molar-based composition calculated from the mass ratio. ^{c} Molar-based composition in the null pressure detector. ^{d} $100(x_{\text{optical cell}} - x_{\text{feed}})/x_{\text{optical cell}}$. ^{e} $100(x_{\text{optical cell}} - x_{\text{null pressure detector}})/x_{\text{optical cell}}$.

Figure 3 shows the experimental results of the four binary systems investigated in this study. The numerical values are tabulated in Tables 4 to 7. As can be seen in the Figure, the spread in the critical density data is wider compared with the critical temperature and pressure. This is presumably due to the characteristics of the critical point where the density changes sharply with only minute changes in temperature and/or pressure. Apparently, the greater the difference in the boiling point and critical temperature, the wider the data spread.

From the Tables, it is also clear that, as described in the Experimental Section, there are composition differences between samples recovered from the optical cell and the null pressure detector. The larger the boiling point and

Table 7. Critical Parameters of HFE-143m (1) + HFC-236ea (2) Systems

$x_1{}^a$	T_C/K	P_C/MPa	ρ_C/kg m^{-3}	$x_1{}^b$ (optical cell base deviation/%)^d	$x_1{}^c$ (optical cell base deviation/%)^e
0.0000	412.41	3.416	562	0.0000 (0.00)	0.0000 (0.00)
0.2452	405.77	3.549	545	0.2467 (−0.61)	0.2431 (0.86)
0.3348	403.16	3.593	541	0.3343 (0.15)	0.3336 (0.36)
0.5434	396.33	3.660	518	0.5459 (−0.46)	0.5455 (−0.39)
0.7338	389.44	3.680	497	0.7337 (0.01)	0.7328 (0.14)
0.8497	384.72	3.687	476	0.8507 (−0.12)	0.8503 (−0.07)
1.0000	377.92	3.640	459	1.0000 (0.00)	1.0000 (0.00)
			AAD/%	0.19	0.26

^{a} Molar-based composition in the optical cell. ^{b} Molar-based composition calculated from the mass ratio. ^{c} Molar-based composition in the null pressure detector. ^{d} $100(x_{\text{optical cell}} - x_{\text{feed}})/x_{\text{optical cell}}$. ^{e} $100(x_{\text{optical cell}} - x_{\text{null pressure detector}})/x_{\text{optical cell}}$.

Table 8. Correlated Results

system	parameters		AAD/%	
HFE-143m + HFC-125	$\Delta_T = 0.6203$		T_C:	0.01
	$\Delta_P = 0.1549$		P_C:	0.08
	$\Delta_V = -4.2630$		ρ_C:	0.67
HFE-143m + HFC-134a	$\Delta_T = -1.9297$		T_C:	0.00
	$\Delta_P = -0.0258$		P_C:	0.08
	$\Delta_V = -4.5938$		ρ_C:	0.42
HFE-143m + HFC-227ea	$\Delta_T = 0.3007$		T_C:	0.01
	$\Delta_P = 0.1416$		P_C:	0.29
	$\Delta_V = -10.5668$		ρ_C:	0.33
HFE-143m + HFC-236ea	$\Delta_T = -2.0074$		T_C:	0.01
	$\Delta_P = 0.2949$		P_C:	0.17
	$\Delta_V = -17.2737$		ρ_C:	0.41

critical temperature difference, the larger the average absolute deviation (AAD) of the composition. This fact suggests that even with the extreme care we took in constructing the apparatus to minimize temperature differences there was still a temperature difference between the optical cell and the null pressure detector. However, because the AAD are smaller than 1% for all four systems investigated, there will be only minor effects on the critical parameters measurements.

Correlation of the Critical Parameters. The correlated results are shown as lines in Figure 3 and are summarized in Table 8. As shown in the Table, the AAD values of the critical parameters are less than ±1%. The AAD values of the critical density are 10 times larger than those of the critical temperature as described above.

Conclusions

We have measured the critical parameters of four binary mixtures of HFE-143m with (i) HFC-125, (ii) −134a, (iii) −227ea, and (iv) −236ea with uncertainties of ±10 mK in temperature, ±0.5 kPa in pressure, and ±1 kg m^{-3} in density. The data spread in the critical density was larger than that of the critical temperature and pressure data. This is presumably due to the difficulty in measuring the density close to the critical point where it changes sharply with only minimal changes in temperature and pressure.

The experimental results were correlated with equations proposed by Higashi.[26,31] The maximum average absolute deviation was less than 1% for all critical parameters. The maximum error was −2% for the density of the HFE-143m + HFC-125 system.

Acknowledgment

Literature Cited

(1) Sekiya, A.; Misaki, S. The potential of hydrofluoroethers to replace CFCs, HCFCs and PFCs. *J. Fluorine Chem.* **2000**, *101*, 215−221.

(2) Ravishankara, A. R.; Turnipseed, A. A.; Jensen, N. R.; Barone, S.; Mills, M.; Howard, C. J.; Solomon, S. Do Hydrofluorocarbons Destroy Stratospheric Ozone? *Science* **1994**, *263*, 71−75.

(3) Research Institute of Innovative Technology for the Earth; *Development of an Advanced Refrigerant for Compression Heat Pumps*; The Research Institute of Innovative Technology for the Earth Report; 1990−1995 (in Japanese; http://www.infoc.nedo.go.jp/udb/dbindex.html).

(4) Research Institute of Innovative Technology for the Earth; *Survey of Alternative Methods and Molecular Design of New Candidate Compounds*; The Research Institute of Innovative Technology for the Earth Report; 1996−2002 (in Japanese; http://www.infoc.nedo.go.jp/udb/dbindex.html).

(5) Sekiya, A.; Yamada, Y. Perspective of the development of new generation refrigerants. *Kotasu-gasu*, **2001**, *38*, 27−31 (in Japanese).

(6) Yasumoto, M.; Yamada, Y.; Murata, J.; Urata, S.; Otake, K. Critical Parameters and Vapor Pressure Measurements of Hydrofluoroethers at High Temperatures. *J. Chem. Eng. Data* **2003**, *48*, 1368−1379.

(7) Otake, K.; Yasumoto, M.; Yamada, Y.; Murata, J.; Urata, S. Critical Parameters and Vapor Pressure Measurements of Potential Replacements for Chlorofluorocarbons−Four Hydrofluoroketones and a Hydrofluoroamine. *J. Chem. Eng. Data* **2003**, *48*, 1380−1383.

(8) Wang, B.-H.; Adcock, J. L.; Mathur, S. B.; van Hook, W. A. Vapor Pressures, liquid molar volumes, vapor nonidealities, and critical properties of some fluorinated ethers: CF$_3$OCF$_2$OCF$_3$, CF$_3$OCF$_2$-CF$_2$H, c-CF$_2$CF$_2$CF$_2$O, CF$_3$OCH$_3$; and of CCl$_3$F and CF$_2$ClH, *J. Chem. Thermodyn.* **1991**, *23*, 699−710.

(9) Salvi-Narkhede, M.; Wang, B.-H.; Adcock, J. L.; van Hook, W. A. Vapor pressures, liquid molar volumes, vapor nonidealities, and critical properties of some partially fluorinated ethers (CF$_3$OCF$_2$-CF$_2$H, CF$_3$OCF$_2$H, and CF$_3$OCH$_3$), some perfluoroethers (CF$_3$-OCF$_2$OCF$_3$, c-CF$_2$OCF$_2$OCF$_2$, and c-CF$_2$CF$_2$CF$_2$), and of CHF$_2$Br and CF$_3$CFHCF$_3$. *J. Chem. Thermodyn.* **1992**, *24*, 1065−1075.

(10) Yoshii, Y.; Widiatmo, J. V.; Watanabe, K. Measurements of critical parameters for HFE-143m. *Rev. High-Pres. Sci. Technol.* **2000**, *10*, 247 (special issue).

(11) Kayukawa, Y.; Widiatmo, J. V.; Watanabe, K. *PVT properties and vapor pressure measurements of HFE-143m and HFE-347 mmy*, Proceedings of Thermophysical Properties 21, Nagoya, Japan, October 18−20, 2000; pp 187−189.

(12) Widiatmo, J. V.; Watanabe, K. *Equations of State for Fluorinated Ether Refrigerants, CF$_3$OCH$_3$ and (CF$_3$)$_2$CFOCH$_3$*, Proceedings of the conference on Thermophysical Properties and Transfer Processes of New Refrigerants, Paderborn, Germany, October 3−5, 2001.

(13) Wilson, L. C.; Wilding, W. V.; Wilson, G. M.; Rowley, R. L.; Felix, V. M.; Chisolem-Carter, T. Thermophysical properties of HFC-125. *Fluid Phase Equilib.* **1992**, *80*, 167−177.

(14) Schmidt, J. W.; Moldover, M. R. Alternative Refrigerants CH$_2$F$_2$ and C$_2$HF$_5$: Critical Temperature, Refractive Index, Surface

Tension, and Estimates of Liquid, Vapor, and Critical Density. *J. Chem. Eng. Data* **1994**, *39*, 39−44.

(15) Kuwabara, S.; Aoyama, H.; Sato, H.; Watanabe, K. Vapor−Liquid Coexistence Curves in the Critical Region and the Critical Temperatures and Densities of Difluoromethane and Pentafluoropropane. *J. Chem. Eng. Data* **1995**, *40*, 112−116.

(16) Nagel, M.; Bier, K. Vapor-Liquid Equilibrium of Ternary Mixtures of the Refrigerants R32, R125, and R134a. *Int. J. Refrig*. **1995**, *18*, 534−543.

(17) Higashi, Y. Vapor−Liquid Equilibria, Coexistence Curve, and Critical Locus for Difluoromethane + Pentafluoroethane (R-32 + R-125). *J. Chem. Eng. Data* **1997**, *42*, 1269−1273.

(18) NIST Reference Fluid Thermodynamic and Transport Properties-REFPROP, v.6.01.

(19) Span, R.; Wagner, W. Equations of State for Technical Application. II. Results for Polar Fluids. *Int. J. Thermodyn*. **2003**, *24*, 111−161.

(20) Maezawa, Y.; Sato, H.; Watanabe, K. Saturated Liquid Densities of HCFC 123 and HFC 134a. *J. Chem. Eng. Data* **1990**, *35*, 225−228.

(21) Baehr, H. D.; Tillner-Roth, R. Measurement and correlation of the vapor pressure of 1,1,1,2-tetrafluoroethane (R 134a) and of 1,1-difluoroethane (R 152a). *J. Chem. Thermodyn*. **1991**, *23*, 1063−1068.

(22) Japan Association of Refrigeration and Japan Flon Gas Association; *Thermophysical Properties of Environmentally Acceptable Fluorocarbons, HFC-134a and HCFC-123*. Tokyo, 1991.

(23) Strom, K. H. U.; Gren, U. B. Liquid Molar Volume of CH_2FCF_3, CH_3CClF_2, and CH_3CHF_2 and the Mixture of $CHFCl_2 + CH_3CClF_2$ and $CHF_2Cl + CH_3CHF_2$. *J. Chem. Eng. Data* **1993**, *38*, 18−22.

(24) Aoyama, H.; Kishizawa, G.; Sato, H.; Watanabe, K. Vapor−Liquid Coexistence Curves in the Critical Region and the Critical Temperatures and Densities of 1,1,1,2-Tetrafluoroethane (R-134a), 1,1,1-Trifluoroethane (R-143a), and 1,1,1,2,3,3-Hexafluoropropane (R-236ea). *J. Chem. Eng. Data* **1996**, *41*, 1046−1051.

(25) Fujiwara, K.; Nakamura, S.; Noguchi, M. Critical Parameters and Vapor Pressure Measurements for 1,1,1-Trifluoroethane (R-143a). *J. Chem. Eng. Data* **1998**, *43*, 55−59.

(26) Higashi, Y., Critical Parameters for HFC134a, HFC32, and HFC125. *Int. J. Refrig*. **1994**, *17*, 524−531.

(27) Shi, K.; Duan, Y.; Zhu, M.; Han, L.; Lei, X., Vapor Pressure of 1,1,1,2,3,3-heptafluoropropane. *Fluid Phase Equilib*. **1999**, *163*, 109−117.

(28) Defibaugh D. R.; Moldover, R. Compressed and Saturated Liquid Densities for 18 Halogenated Organic Compounds. *J. Chem. Eng. Data* **1997**, *42*, 160−168.

(29) Defibaugh, D. R.; Gillis, K. A.; Moldover, R.; Schmidt, J. W.; Webber, L. A. Thermodynamic Properties of $CF_3-CHF-CHF_2$, 1,1,1,2,3,3-hexafluoropropane. *Fluid Phase Equilib*. **1996**, *122*, 131−155.

(30) Zhang, H.-L.; Sato, H.; Watanabe, K. Vapor Pressure Measurements of 1,1,1,2,3,3-Hexafluoropropane from 300 to 410 K. *J. Chem. Eng. Data* **1995**, *40*, 1281−1284.

(31) Higashi, Y. Vapor-Liquid Critical Surface of Ternary HFC-32-(CH_2F_2) + HFC-125(CF_3CHF_2) + HFC-134a(CF_3CH_2F). *Int. J. Thermophys*. **1999**, *20*, 1483−1495.